Translational Oncology 69 (2026) 102805

Contents lists available at ScienceDirect

Translational Oncology

journal homepage: www.elsevier.com/locate/tranon

Single-cell RNA sequencing reveals immune microenvironment heterogeneity in BRCA1-mutated and sporadic triple-negative breast cancer

Qi Sun [a,1], Yuting Zhong [b,1], Changgang Sun [a,c,d,*]

[a] College of First Clinical Medicine, Shandong University of Traditional Chinese Medicine, Jinan, Shandong, 250000, China
[b] School of Integrative Medicine, Shanghai University of Traditional Chinese Medicine, Shanghai 201203, China
[c] College of Traditional Chinese Medicine, Shandong Second Medical University, Weifang, Shandong, 261000, China
[d] Department of Oncology, Weifang Traditional Chinese Hospital, Weifang, Shandong, 261000, China

ARTICLE INFO

Keywords:
Triple-negative breast cancer
BRCA1 mutation
Single-cell RNA sequencing
Tumor immune microenvironment
B cells
Biomarkers

ABSTRACT

Immune checkpoint blockade has shown benefit in some Triple-negative breast cancer (TNBC) patients, but responses are variable. BRCA1-mutated TNBC represents a biologically distinct subgroup, potentially differing in immunogenicity and immunotherapy responsiveness. However, immune microenvironment differences between BRCA1-mutated and sporadic TNBC remain incompletely understood. By performing single-cell RNA sequencing analysis on sporadic TNBC and BRCA1 mutant TNBC, we assessed immune cell composition, transcriptional program, pathways, stemness, differentiation, and transcription factor regulatory networks. B cell and plasma cell subtypes were further explored using AUCell, CytoTRACE, Monocle2, and Slingshot. Compared to sporadic TNBC, BRCA1-mutated TNBC exhibited a distinct immune landscape with enriched naïve and memory B cells, while sporadic TNBC was dominated by terminally differentiated plasma cells, including IgA plasma cells. Functional enrichment analyses showed enhanced adaptive immune signaling, antigen presentation, and B cell receptor pathways in BRCA1-mutated TNBC, while sporadic TNBC had humoral effector and immunoregulatory programs. Trajectory and stemness analyses indicated enhanced cellular plasticity and decreased differentiation in B cells derived from BRCA1-mutated triple-negative breast cancer. Analysis of transcription factors revealed JUND and ETV1 in BRCA1-mutated TNBC, and MEIS1 and CEBPB in sporadic TNBC. Our findings underscore disparities in the immune ecosystem between BRCA1-mutated and spontaneous TNBC, indicating that the B cell-centric immunological milieu in BRCA1-mutated TNBC may offer a more advantageous setting for immunotherapy. Sporadic TNBC, by contrast, exhibits an immunological state characterized by plasma cells, which may restrict immune reactivation. These data indicate that B cell-based immunological stratification may guide precision immunotherapy approaches.

Introduction

Triple-negative breast cancer (TNBC) lacks specific targeted treatment options due to the absence of estrogen receptor, progesterone receptor, and HER2 expression [1,2]. Its highly aggressive nature and poor prognosis make it one of the major challenges in clinical treatment [3,4]. The intrinsic molecular heterogeneity and dynamic regulation of the tumor immune microenvironment (TME) in TNBC form a crucial basis for its heterogeneous therapeutic response [5–8]. In recent years, immune checkpoint inhibitors (ICIs) have progressively established their role in TNBC therapy. Their introduction offers novel strategies for treating this refractory disease [9–13]. TNBC generally demonstrates increased numbers of tumor-infiltrating lymphocytes (TILs) and PD-L1 expression, which, along with its heightened tumor mutational burden, indicates enhanced immunogenicity [14–17]. Despite this, only a subset of TNBC patients achieve durable responses or significant survival benefits from ICIs therapy [18,19]. Responses to immune therapy in TNBC are highly heterogeneous, and monotherapy yields limited overall survival benefits in previously treated populations [20], suggesting that the receptor-level classification of TNBC masks fundamental differences in immune ecosystems [21,22].

Within the genetic heterogeneity of TNBC, BRCA1 mutations constitute a subgroup with unique biological traits [23]. BRCA1-mutated TNBC is thought to exhibit distinct molecular

* Corresponding author to: College of First Clinical Medicine, Shandong University of Traditional Chinese Medicine, Jinan, Shandong, 250000, China.
E-mail address: 2023100062@sdutcm.edu.cn (C. Sun).
[1] Qi Sun and Yuting Zhong contributed equally to this work.

https://doi.org/10.1016/j.tranon.2026.102805
Received 2 March 2026; Received in revised form 18 April 2026; Accepted 30 April 2026

mechanisms concerning immunotherapy in contrast to non-mutated triple-negative breast cancer [24]. Genomic instability arising from homologous recombination deficiency and the consequent rise in neoantigens may augment tumor immunogenicity, thereby enhancing the efficacy of immunotherapy. Conversely, clinical combination therapy utilizing PARP inhibitors and immunotherapy has shown efficacy in triple-negative breast cancer, especially in individuals with BRCA mutations or homologous recombination deficiency. Research indicates that the combination of niraparib and pembrolizumab yields significant disease control rates in advanced or metastatic TNBC, with response rates notably elevated in BRCA-mutated tumors [25]. These findings suggest that BRCA-mutated TNBC not only exhibits greater immunogenicity but also possesses an immune microenvironment structure potentially better suited for “reactivation” by ICIs.

With the maturation of single-cell RNA sequencing (scRNA-seq) technology, researchers can now resolve the complex heterogeneity of the TME at single-cell resolution [26–29]. scRNA-seq systematically delineates discrete subpopulations of immune cells and their associated transcriptional states [30], which is essential for comprehending the properties and roles of immune cells in TNBC. Current research has employed scRNA-seq to create comprehensive maps of the breast cancer tumor microenvironment, revealing various immune cell populations, unique NK cell statuses, and intricate immune regulatory pathways [31]. These studies illustrate the significant variability of immune cell composition and functional states within the tumor microenvironment [32]. Particularly in TNBC, scRNA-seq analyses reveal substantial heterogeneity in immune cell lineages across distinct TNBC subtypes, closely associated with tumor progression, immune activation, or immunosuppression programs [33].

Although existing single-cell studies have revealed the complexity of the TNBC immune microenvironment, systematic comparisons of differences in immune composition, immune status, and immunotherapy sensitivity between common TNBC and BRCA1-mutated TNBC remain insufficient [34]. The fundamental distinctions between the immune ecosystem structure of BRCA1-mutated TNBC and that of common TNBC lack in-depth analysis. In this context, doing comparative analyses utilizing extensive single-cell immunoscale data to discern variations in immune cell composition, functional states, and differentiation pathways between typical TNBC and BRCA1-mutant TNBC is critically important. This not only aids in revealing the mechanistic factors underlying the disparate responses to immunotherapy between the two TNBC subtypes but may also provide theoretical foundations and potential biomarkers for TNBC immune subtyping and precision immunotherapy strategies.

Methods

Single-cell sequencing data sources

The scRNA-seq data used in this study were obtained from the Gene Expression Omnibus database [35], with the dataset identifier GSE161529. This dataset comprised single-cell transcriptome sequencing data from breast cancer patients, covering multiple molecular subtypes of breast cancer. It involved systematic collection and sequencing of tumor tissues and corresponding control samples. All data used in this study can be accessed without restriction.

scRNA-seq data processing

The analysis was performed using the Seurat R package (version 4.4.0) [36,37]. Quality control was conducted utilizing the DoubletFinder R package (version 2.0.3) [38]. Subsequently, gene expression matrices for the remaining cells were generated using logarithmic normalization and linear regression techniques, utilizing the "NormalizeData" and "ScaleData" functions from the Seurat R package (version 4.4.0) [39]. The "FindVariableFeatures" function was then applied to identify the top 2000 most variable genes and perform principal component analysis [40]. The Harmony package (version 1.2.0) was employed for batch effect correction [41].

Determination of cell and pathway enrichment analysis

Cell clusters were initially identified using the "FindNeighbors" and "FindClusters" functions implemented in Seurat [42]. The Seurat "FindAllMarkers" function was used to conduct the Wilcoxon rank-sum test for the assessment of differentially expressed genes (DEGs) across various cellular clusters [43].

Enrichment analyses of DEGs in various cell types were conducted using Gene Ontology (GO) and Gene Set Enrichment Analysis (GSEA) (http://software.broadinstitute.org/gsea/msigdb) tools using ClusterProfiler R package (version 4.14.0) [44].

Developmental trajectory inference

Cell differentiation trajectories were constructed with Monocle R package (version 2.24.0) [45]. Visualization facilitated by the "plot_cell_trajectory" function. The different cell subpopulations were then sorted based on their pseudotime order.

The slingshot R package (version 2.10.0) was used for inferring cell lineages and pseudotime. The "getCurves" function was employed to obtain smoothed trajectory curves.

SCENIC analysis

To calculate the regulon activity scores of cells, we used the SCENIC R package (version 0.10.0) within the Python (version 3.7) for SCENIC analysis. First, GRNBoost2 was used to infer the co-expression modules between transcription factor (TFs) and candidate target genes. Then, RcisTarget was used to analyze the genes in each co-expression module to identify the enriched motifs (a TF and its potential direct target genes were defined as a regulon). The AUCell method was applied to quantify regulon activity at the single-cell level.

Statistical analysis

R software and Python software were used for database data analysis. All mentioned p-values were two-tailed, with values below 0.05 considered statistically significant. Values below 0.001 were deemed highly significant, while those below 0.0001 were considered extremely significant.

Results

Construction of a comprehensive single-cell atlas of the breast immune microenvironment

To obtain a comprehensive single-cell atlas of the breast immune microenvironment, we collected single-cell sequencing data from 17 ER+ tumors (T-ER), 6 HER+ tumors (T-HER2), 1 PR+ tumor (T-PR), 4 TNBCs (TN), and 4 BRCA1+ TNBCs (TN-BRCA1) from 52 patients, as well as whole-breast cells from 13 healthy controls without breast cancer and normal epithelial breast cells from 11 patients (HC). After quality control and filtering of the sequencing data, 295,804 cells were obtained. Following unsupervised clustering and reference to classical cellular markers, these cells were classified into nine cell types: epithelial cells (EPCs), T and NK cells, fibroblasts, smooth muscle cells, myeloid cells, endothelial cells (ECs), B and Plasma cells, pericytes, and mast cells (MCs)(Fig. 1A). Fig. 1B showed the distribution of these nine cell types and different tissue origins on UMAP, while also displaying the proportion of cells in the cell cycle and grouping across the nine cell types. EPCs, myeloid cells, ECs and Fibroblasts exhibited a higher proportion of cells in the G1 phase, indicating a relatively quiescent

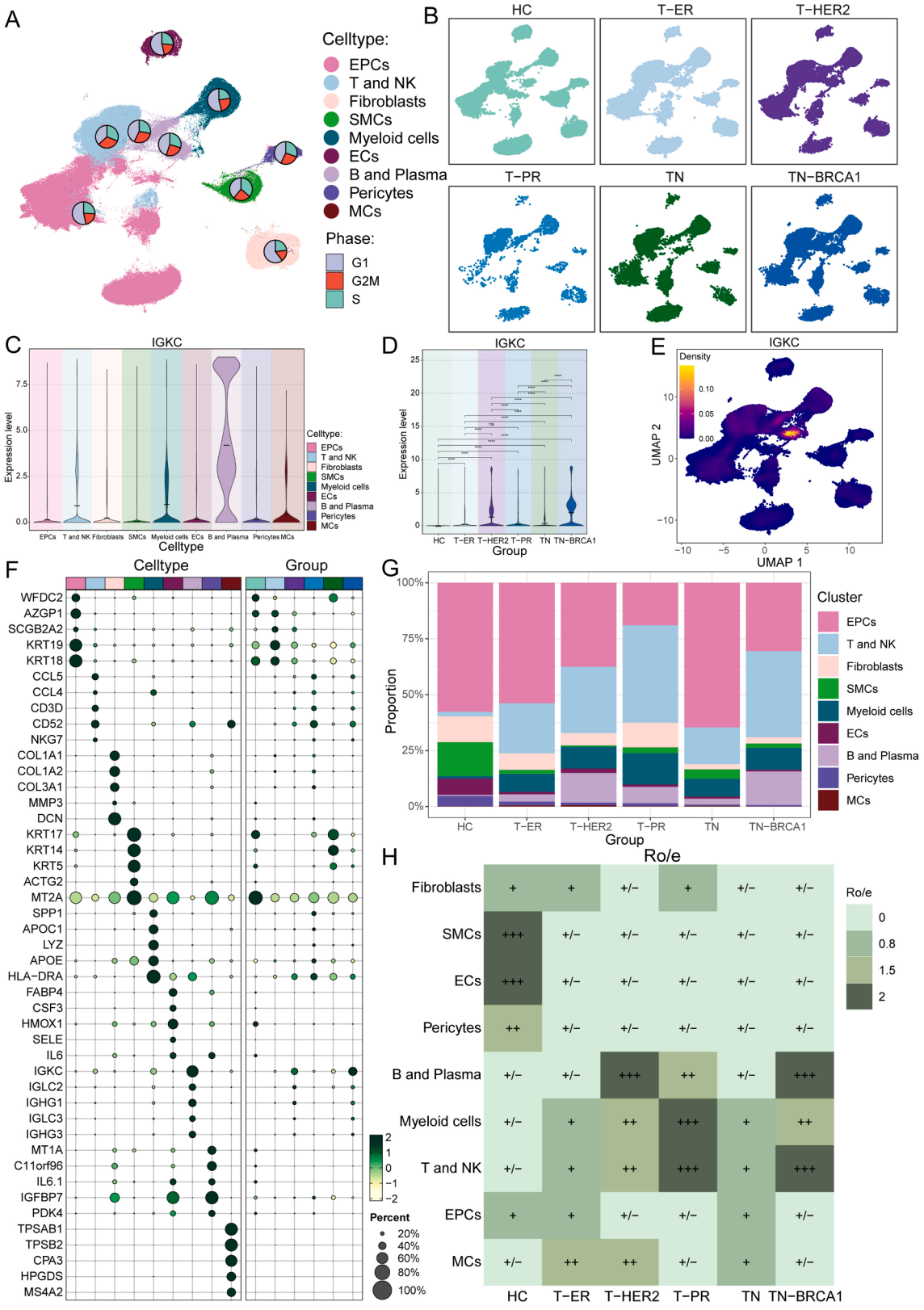

Figure 1. Single-cell landscape of breast tumors and normal tissues. (A) UMAP clustering plot, with pie charts showing the cell phase scores from RNA sequencing. (B) UMAP plot showing the clustering of different groups. (C) Violin plots showing the expression levels of IGKC across different cell types. (D) Violin plots showing the expression levels of IGKC across different groups, where *** indicates $P < 0.001$ and ns indicates no statistically significant difference. (E) UMAP plot showing the expression density distribution of the IGKC gene in the single-cell UMAP embedding. (F) Bubble plots showing the differential expression of the top 5 marker genes across cell types and tissue origins. (G) Stacked bar charts showing the proportion of each cell type in different groups. (H) Heatmap of Ro/e scores used to evaluate the tissue origin preference of different cell types.

transcriptional state rather than active proliferation. Conversely, B and Plasma cells exhibited a higher proportion in the G2/M phase, consistent with a proliferative cellular state, potentially indicated the presence of tumor immune responses within the microenvironment. To validate the accuracy of our cell type annotation, we visualized *IGKC*, one of the classic markers for B and Plasma cells (Figs. 1C-E). *IGKC* was differentially highly expressed in B and Plasma cells, and we observed its nearly complete absence in both the HC and TN groups, while it exhibited high expression levels in the T-HER2 and TN-BRCA1 group. Fig. 1F further demonstrated the top five markers for all cell types, consistent with their biological context. Additionally, the stacked proportion plots and tissue preference maps revealed that breast cancer tumor tissues exhibited significant immune infiltration compared to normal tissues, with markedly increased proportions of T and NK cells and B and Plasma cells, these cells also demonstrated a preference for different tumor types. (Figs. 1G-H). The proportions of immune cells also varied within different tumor types. B and Plasma cells, T and NK cells, and myeloid cells were all significantly enriched in T-HER2, T-PR, and TN-BRCA1 tissues, while T-ER and TN tissues show comparatively lower levels. Notably, although both TN and TN-BRCA1 belong to the TNBC spectrum, their immune infiltration patterns were clearly distinct, indicating that different molecular backgrounds within TNBC may shape divergent immune microenvironments. Thus, the differences in the immune microenvironment between the TN and TN-BRCA1 groups particularly caught our attention.

Functional characterization of major cell types in the breast tumor microenvironment

Next, we performed DEGs analysis and enriched pathway analysis on the nine cell types obtained from breast tissue samples, and present the results (Fig. 2A). In EPCs, elevated expression of mitochondrial respiratory chain complex I genes, including *NDUFA1, NDUFC2*, and *NDUFB6*, signifies a substantial enhancement in mitochondrial energy metabolism mostly driven by oxidative phosphorylation (*NDUFC2*). This signified their heightened metabolic requirements and functional activity, presumably providing sustained energy support for tumor epithelial cells during proliferation, biosynthesis, and adaptation to the microenvironment. In B and Plasma cells, genes like *HLA-DRB1* [46], *CD74* [47], and *PTPRC* exhibited significant activation, indicating that this cell type possesses distinct antigen-presenting capabilities and mature immune cell characteristics. In myeloid cells, inflammatory and innate immunity-related genes, including *TNF* and *TLR4*, were markedly activated, alongside elevated expression of the immune regulating receptor *TREM2*. This indicated that this cell population is in a functional state marked by simultaneous inflammatory activation and immunological control. In T and NK cells, immunological activation and effector-related genes, including *PTPRC* and *IFNG*, were markedly elevated, alongside increased *HMGB1* activity, indicating that this population is in a highly activated effector state with the capacity for inflammatory amplification . Following this, we presented the pathway enrichment of each cell type in the GO-BP entries, highlighting the three immune cell types of interest separately (Figs. 2B-C). All three were enriched in pathways related to immune activation and regulation, such as “lymphocyte activation”, “regulation of immune response”, and “immune effector process”. We performed GSEA to visualize pathways associated with B and Plasma cells exhibiting significant proportion differences between the TN and TN-BRCA1 groups (Fig. 2D). Results demonstrated that B and Plasma cells dramatically enriched and elevated various pathways linked to adaptive immunity, including "adaptive immune response," "BCR signaling," "antigen processing and presentation," and "immunoglobulin production." In contrast, pathways linked to “neutrophil chemotaxis” and “granulocyte migration” demonstrated a downregulated trend, indicating that this B and Plasma cell population displays a pronounced inclination towards humoral immunity and antigen presentation functions, while innate immune chemotactic mechanisms associated with granulocyte recruitment were comparatively reduced. The adaptive immunological features, mostly influenced by B and Plasma cells, identified in the TN and TN-BRCA1 cohorts may elucidate their varied responses to immunotherapy, underscoring the significance of B cell-mediated immune control in TNBC.

B and plasma cell heterogeneity underlies differential immune landscapes in TN and TN-BRCA1 tumors

The preceding analysis piqued our interest in B and Plasma cells. Therefore, we performed dimensionality reduction clustering specifically on B and Plasma cells from the TN and TN-BRCA1 groups, identifying 2 naïve B cell subtypes, 2 memory B cell subtypes, 9 IgG plasma cell subtypes, and 1 IgA plasma cell subtype (Fig. 3A). We then used a faceted plot to visualize the UMAP-based dimensionality reduction distributions of the two TNBC subtypes and different TNBC patients (Figs. 3B-C). Fig. 3D illustrated the five principal marker genes for each B and Plasma cell subtype. Plasma cells were chiefly defined by immunoglobulin-associated genes, whereas naïve B cells and memory B cells are mainly distinguished by immunological activation-associated genes. Next, we analyzed and visualized the enrichment differences between the two groups (Fig. 3E). Notably, the TN group primarily enriched genes highly associated with plasma cells, while the TN-BRCA1 group enriched genes associated with naïve B cells. To further identify biological distinctions between these two groups, we visualized the distribution proportions of these B and Plasma subtypes across different groups (Figs. 3F-G). It was evident that C0 *CD83*+ Naïve B cells, C2 *MS4A1*+ Memory B cells, C4 *CD69*+ Naïve B cells, *and* C7 *CD52*+ Memory B cells were significantly more prevalent in the TN-BRCA1 group compared to the TN group. Conversely, the TN group exhibited a higher proportion of plasma cells(Fig. 3H). Overall, TN-BRCA1 tumors exhibited an immune composition characterized primarily by naïve/memory B cell expansion and activation-related phenotypes, whereas TN tumors tended toward a humoral effector state associated with terminal B cell differentiation.

Functional pathway enrichment analysis reveals heterogeneity among B and plasma cell subtypes

Next, we presented the DEGs obtained from four cell subtypes derived from B and Plasma cells: C0 *CD83*+ Naïve B cells, C1 *MZB1*+ IgG plasma cells, C2 *MS4A1*+ memory B cells, and C9 *IGHA2*+ IgA plasma cells (Fig. 4A). Each B and Plasma cell subtype demonstrated transcriptional features that align with its cellular identity at the level of DEGs. In C0 *CD83*+ Naïve B cells, *CD69* and *CD83* exhibited upregulation, but *XBP1* and *MZB1*, linked to plasma cell development and secretory pathways, demonstrated downregulation, indicating that this population signifies active, antigen-presenting naïve-like B cells. C2 *MS4A1*+ Memory B cells demonstrated an increase of *MS4A1* and a downregulation of *MZB1*, aligning with the characteristics of mature non-plasma cell lineage B cells. Conversely, plasma cell subtypes exhibited isotype-specific immunoglobulin expression: C1 *MZB1*+ IgG plasma cells upregulated *IGHG3/IGHGP* and downregulated *MS4A1*, whereas C9 *IGHA2*+ IgA plasma cells upregulated *IGHA2* and *JCHAIN* while downregulating *IGHG4*, thereby reinforcing the molecular characterization of IgG and IgA plasma cells. At the enriched route level, these four subgroups equally displayed traits aligned with their biological contexts (Fig. 4B). C0 *CD83*+ Naïve B cells and C2 *MS4A1*+ Memory B cells have enhanced activity in leukocyte and immunological-related pathways, indicating their principal role in immune recognition, antigen presentation, and the control of adaptive immunity. C1 *MZB1*+ IgG plasma cells and C9 *IGHA2*+ IgA plasma cells demonstrated increased activity in endoplasmic reticulum-associated pathways, indicative of their robust protein synthesis and antibody production capabilities. Applying this characteristic to further subtypes of the same

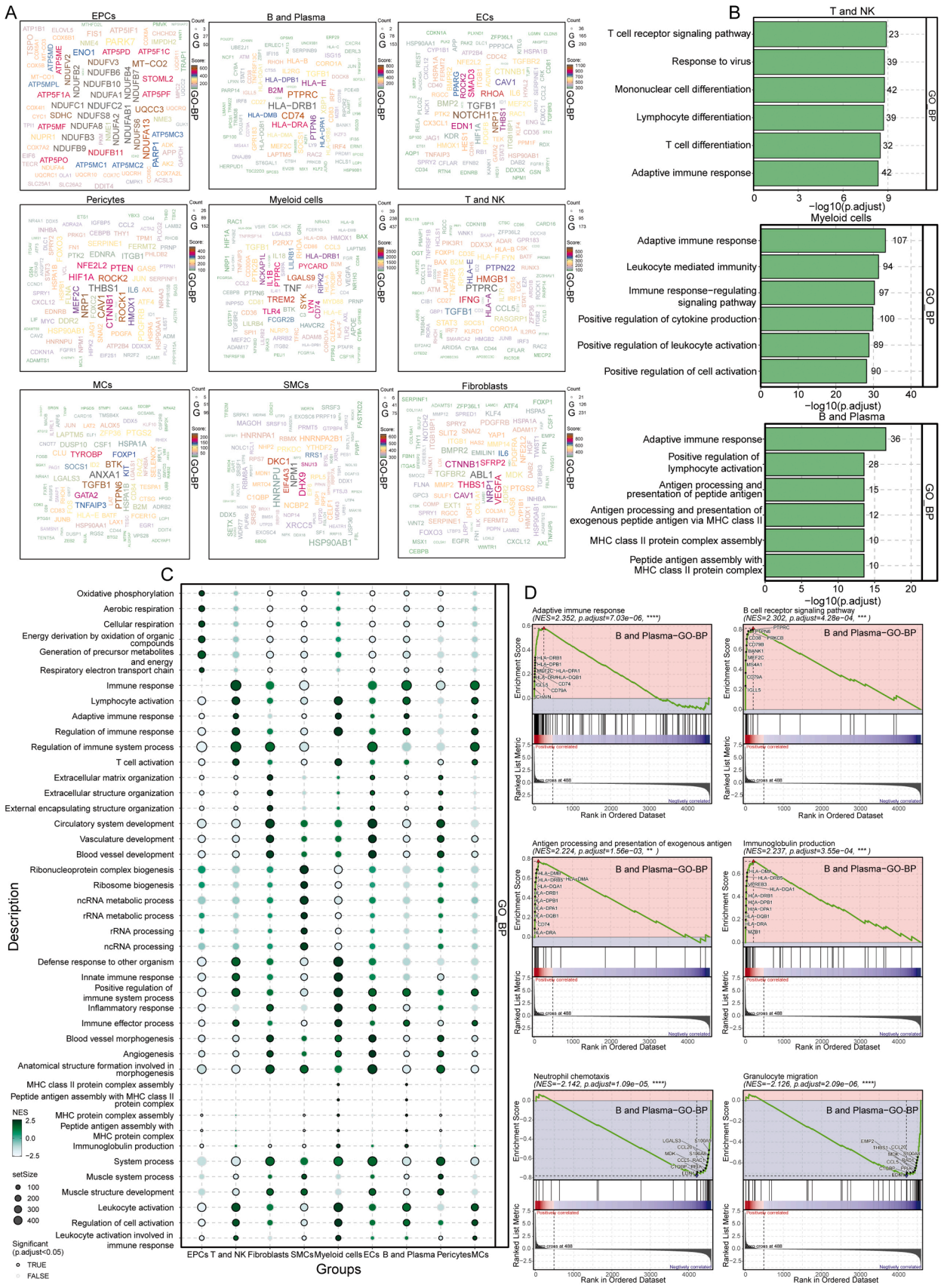

Figure 2. Cell-type-specific transcriptional programs reveal immune activation heterogeneity across breast cancer subtypes. (A)Word cloud plots intuitively show the core marker genes and their functional pathway preferences across different cell types. (B) Bar plots of GO-BP enrichment analysis for T and NK cells, myeloid cells, and B and Plasma cells. (C) Bubble plots showing the GO-BP pathway enrichment analysis across different cell types. (D) GSEA plot of immune pathways in B and Plasma cells.

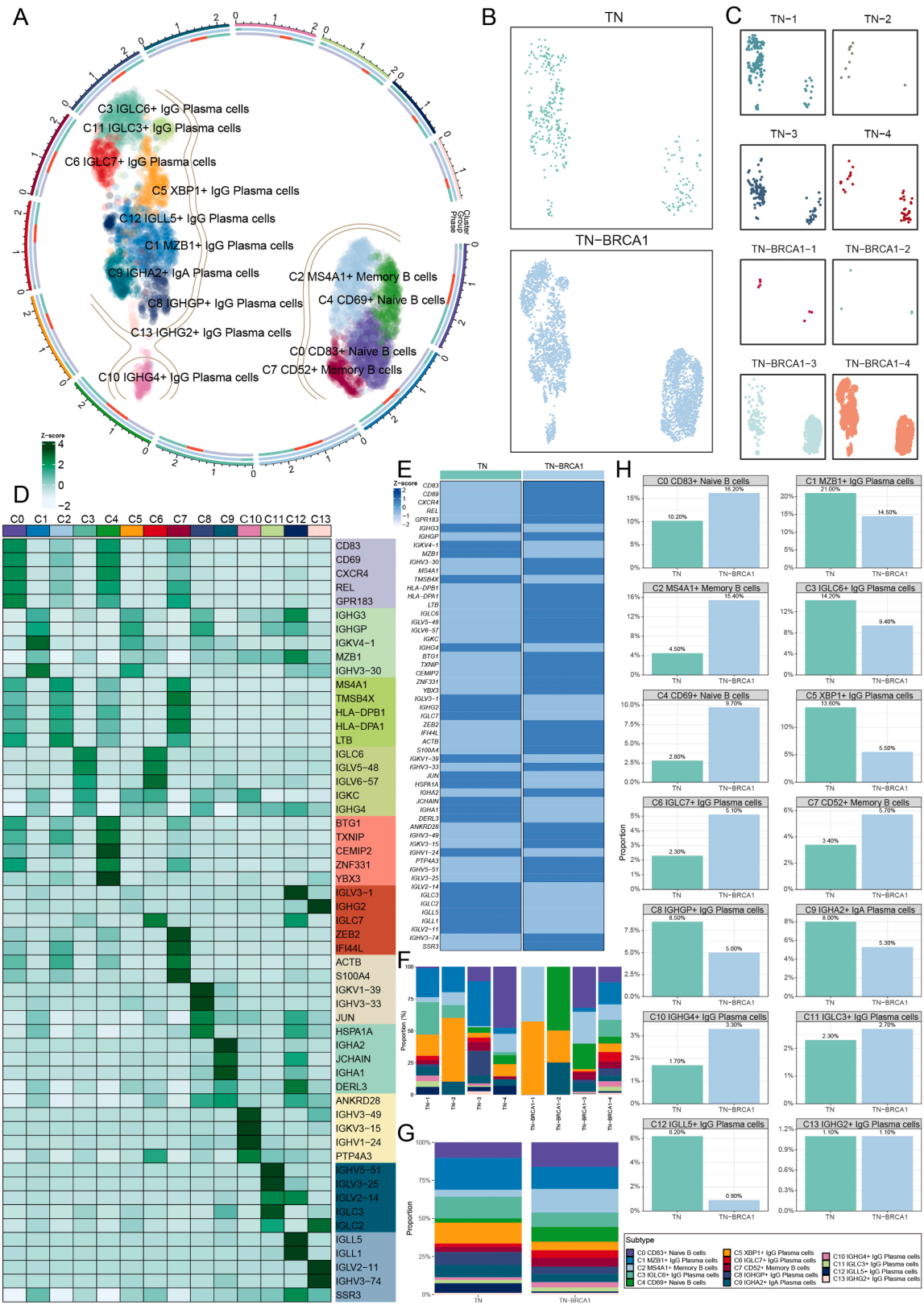

Figure 3. Heterogeneity and subtype composition of B and Plasma cells in TN and TN-BRCA1 tumors. (A) Single-cell circular clustering plot of the B and Plasma cell lineage. (B) UMAP clustering of the TN and TN-BRCA1 groups. (C) UMAP plots showing the clustering of 8 triple-negative breast cancer samples. (D) Heatmap showing marker genes of 14 B and Plasma cell subtypes. (E) Heatmap showing DEGs of the TN and TN-BRCA1 groups. (F) Stacked bar plot of cell proportions across 8 sample group. (G) Stacked bar plot of cell type proportions in TN and TN-BRCA1 samples. (H) Bar graphs showing the proportions of different B and Plasma cell subtypes in TN and TN-BRCA1 groups.

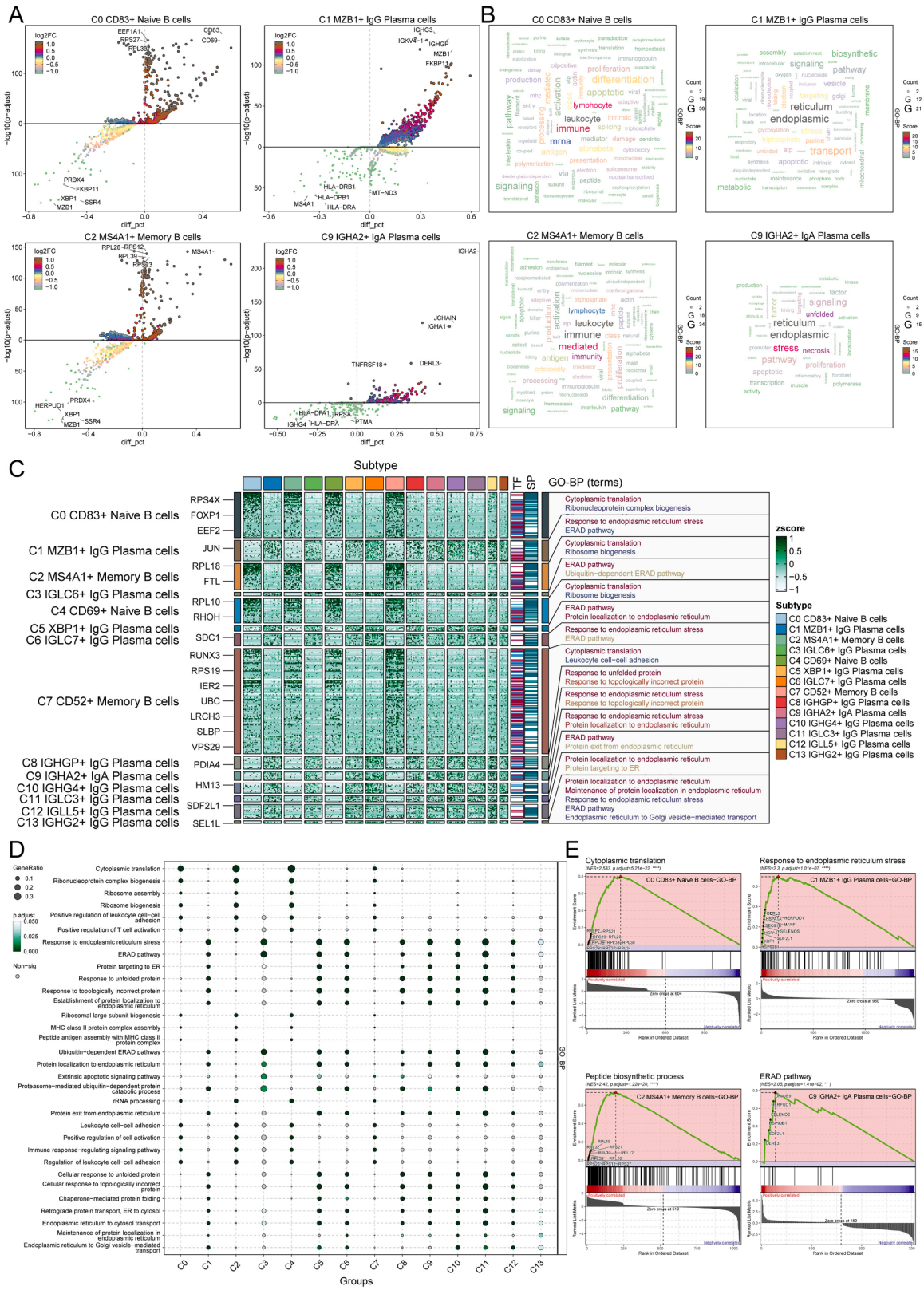

Figure 4. Pathway enrichment characteristics of B and Plasma cell subtypes. (A) Volcano plots illustrated the DEGs in four B and Plasma cell subtypes (C0 CD83⁺ Naïve B cells, C1 MZB1⁺ IgG plasma cells, C2 MS4A1⁺ memory B cells, and C9 IGHA2⁺ IgA plasma cells). (B) Word cloud showing the gene expression levels in C0, C1, C2, and C9 cell subtypes. (C) Heatmap of characteristic gene expression patterns and corresponding GO-BP enrichment results across 14 B and Plasma cell subtypes. (D) Bubble plot displaying the pathway enrichment results of 14 B and Plasma cell subtypes. (E) GSEA plots of key biological processes in four representative B and Plasma cell subtypes(C0 CD83⁺ Naïve B cells, C1 MZB1⁺ IgG plasma cells, C2 MS4A1⁺ memory B cells, and C9 IGHA2⁺ IgA plasma cells).

category produced uniform outcomes (Figs. 4C-E). Memory B cells and naïve B cells significantly enhance pathways linked to cytoplasmic translation, indicating they are in an active state primarily dedicated to manufacturing proteins related to immune activity. Conversely, plasma cells markedly enhanced pathways associated with the endoplasmic reticulum and endoplasmic reticulum-associated degradation, signifying their highly active state of antibody synthesis and dependence on endoplasmic reticulum-associated protein quality control mechanisms to sustain secretory homeostasis. These findings indicated functional variations in protein synthesis and secretion patterns during different stages of B and Plasma cell development.

Subtype-specific stemness features reveal differential B and plasma cell state plasticity in TN and TN-BRCA1 tumors

After defining the functional characteristics of different B and Plasma cell subtypes, we further assessed their state features from the perspective of cell stemness to explore differences in cellular differentiation potential between TN and TN-BRCA1 tumors. We first scored cell stemness using AUC (Fig. 5A). Although no significant difference in overall cellular pluripotency AUC scores was observed between the TN and TN-BRCA1 groups, elevated expression levels of multiple pluripotency-related genes (such as *CD44, CTNNB1*, and *HIF1A*) were detected in memory B cells and naïve B cells (Figs. 5B-C). *CD44, CTNNB1*, and *HIF1A* respectively indicated cellular state plasticity and non-terminal differentiation traits via cell adhesion and migration, differentiation regulation, and microenvironment adaption. The markedly elevated proportion of these B and Plasma cell subtypes in the TN-BRCA1 group indicates that TN-BRCA1 malignancies may contain enriched populations of B and Plasma cell exhibiting greater state flexibility. Immunological cell stated displaying these properties are acknowledged as factors in prolonged immunological activation and antigen presentation [48]. These factors were increasingly recognized in the context of immune therapy responses in triple-negative breast cancer. Despite the absence of a notable difference in overall stemness scores between the TN and TN-BRCA1 groups, the concentration of pertinent gene programs in particular B and Plasma cell subtypes indicated that the plasticity of immune cell states may influence the variability of immune treatment responses in TNBC. Subsequently, we evaluated the differentiation status of B and Plasma cell subtypes with CytoTRACE (Fig. 5D). The results indicated notable disparities in differentiation levels among several B cell subtypes, with C4 *CD69*+ Naïve B cells displaying the highest CytoTRACE scores. This indicated that this subtype may exist at an initial phase of the B and Plasma cell differentiation pathway, marked by less differentiation and increased state flexibility. In conclusion, while no notable differences in overall cellular pluripotency scores were detected between the TN and TN-BRCA1 groups, subtype analysis revealed that naïve B cells and memory B cells demonstrated elevated expression of pluripotency-associated genes and CytoTRACE scores, indicating reduced differentiation and enhanced state plasticity. Conversely, plasma cells exhibited signs of terminal differentiation. In light of these findings, we subsequently performed trajectory and differentiation analyses to thoroughly delineate the dynamic shift of B and Plasma cells from initial stages to terminally differentiated states.

Monocle2 and slingshot studied highlight continuous paths of B and plasma cell development

We comprehensively examined the ongoing process of B and Plasma cell development from naïve/Memory states to IgG/IgA plasma cells using Monocle2 and Slingshot trajectory analysis methods. Monocle2 analysis in Figs. 6A-B revealed that subtypes C0, C2, C4, and C7 reside on early branches of the differentiation trajectory, representing the naïve/Memory B cell stage; subtype C1 occupies the mid-stage of the trajectory, while all other plasma cell subtypes were located at the terminal differentiation stage. Subsequent Slingshot analysis revealed four rather autonomous differentiation lineages (Figs. 6C-D). All lineages arose from the C4 *CD69*+ Naïve B cell subtype and progress via an intermediate C1 state, indicating that C4 may function as the initiation point for differentiation, whereas C1 signified a common transitional phase in B cell-to-plasma cell maturation. The principal distinction across lineages resided in their differentiation endpoints: The lineage culminated in the C9 IgA plasma cell subtype, whereas the other three lineages concluded in the IgG plasma cell subtype. Consequently, lineage 2 was chosen as the representative trajectory for characterizing IgG plasma cell differentiation. Lineage 1 directly differentiates into C9 IgA plasma cells after progressing through C1, while lineage 2 successively differentiates into C5 IgG plasma cells before ultimately reaching C11 IgG plasma cells. Fig. 6E illustrated the dynamic alterations in the expression of memory B cell markers *MS4A1* and *CD52*, naïve B cell marker *CD69*, and IgG plasma cell marker *IGHG2* throughout the differentiation process. *MS4A1, CD69*, and *CD52* all showed significant increases at early stages of the trajectory before declining later. Conversely, *IGHG2* gradually increased during the later stages. Furthermore, we compared the functional pathway dynamics of lineage 1 and lineage 2 during differentiation trajectories (Fig. 6F). Enriched pathways in the early differentiation stage primarily involved junctions and actin, whereas later stages featured pathways related to the endoplasmic reticulum. This further reflected the shift in B and Plasma cell from immune regulatory functions to high-level antibody secretion capabilities during differentiation.

Transcription factor heterogeneity in B and plasma cell reflects distinct immune regulatory landscapes in TN and TN-BRCA1 tumors

To explore the potential molecular basis underlying the differential immunotherapy response between TN and TN-BRCA1, we performed a visualization analysis of TFs differences across subtypes and groups within B and Plasma-related cell subtypes (Fig. 7A). The results indicated that naïve and memory B cells displayed highly analogous transcription factor expression profiles, whereas various plasma cell subtypes demonstrated relatively uniform transcription factor characteristics, implying that the differentiation stage of B and Plasma cells is the principal factor influencing their transcriptional regulatory programs. At the subtype level, naïve/memory B cells typically overexpressed transcription factors including *REL, IRF8*, and *EGR3*, which were intricately linked to B and Plasma cell activation, immune response modulation, and differentiation plasticity. Conversely, plasma cell subtypes markedly overexpreseds transcription factors such as *PRDM1, XBP1*, and *JUN*, aligning with their traits of terminal differentiation and active antibody secretion pathways. Subsequent intergroup comparative study indicated markedly increased *MEIS1* and *CEBPB* expression in the TN group, whereas the TN-BRCA1 group exhibited enhanced *JUND* and *ETV1* expression, implying divergent B and Plasma cell transcriptional regulatory networks between the two groups (Fig. 7B). *MEIS1* expression was significantly elevated in C9 IgA plasma cells compared to other B and Plasma cell subtypes, indicating a possible correlation with differentiation or functional states unique to IgA plasma cells. Prior research suggested that IgA plasma cells may have unique functions in the tumor immunological milieu, in contrast to IgG-dominant humoral immune responses [49]. IgA was generally linked to mucosal immune responses, prioritizing immunological control rather than direct cytotoxicity. In the context of tumors, augmented IgA responses has been observed to correlate with characteristics of an immunosuppressive milieu, potentially affecting myeloid cell function and T cell-mediated antitumor immunity [50,51]. The proliferation of IgA plasma cells in the TN group and the elevated expression of the particular transcription factor *MEIS1* indicated a potential bias in B and Plasma cell development towards IgA production states. This differentiation bias may shape unique immune regulatory patterns and alter responses to immune checkpoint inhibitor therapy, however its exacted functional relevance

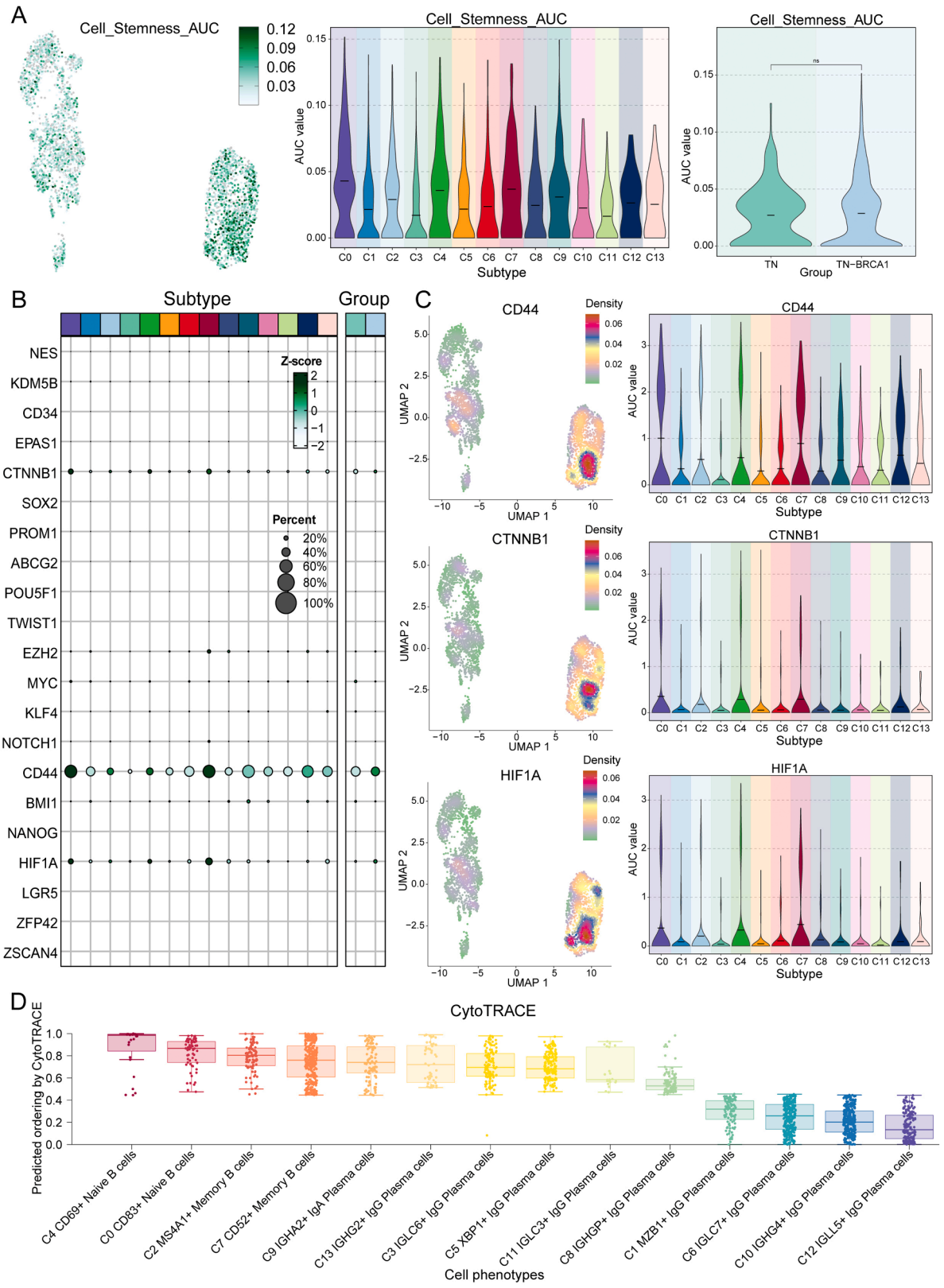

Figure 5. Stemness characteristics of B and Plasma cell subtypes. (A) The distribution of cell stemness scores (cell stemness AUC) was visualized via single-cell UMAP plots and violin plots, with violin plots further showing the cell stemness score differences between the two groups. (B) Bubble plot showing the expression of stemness-related marker genes across 14 distinct B and Plasma cell subtypes and 2 groups. (C) UMAP clustering plots and violin plots showing the density of CD44, CTNNB1, HIF1A genes and their expression levels across 14 B and Plasma cell subtypes, respectively. (D) Box plot showing B and Plasma cell subtypes arranged according to the CytoTRACE prediction order.

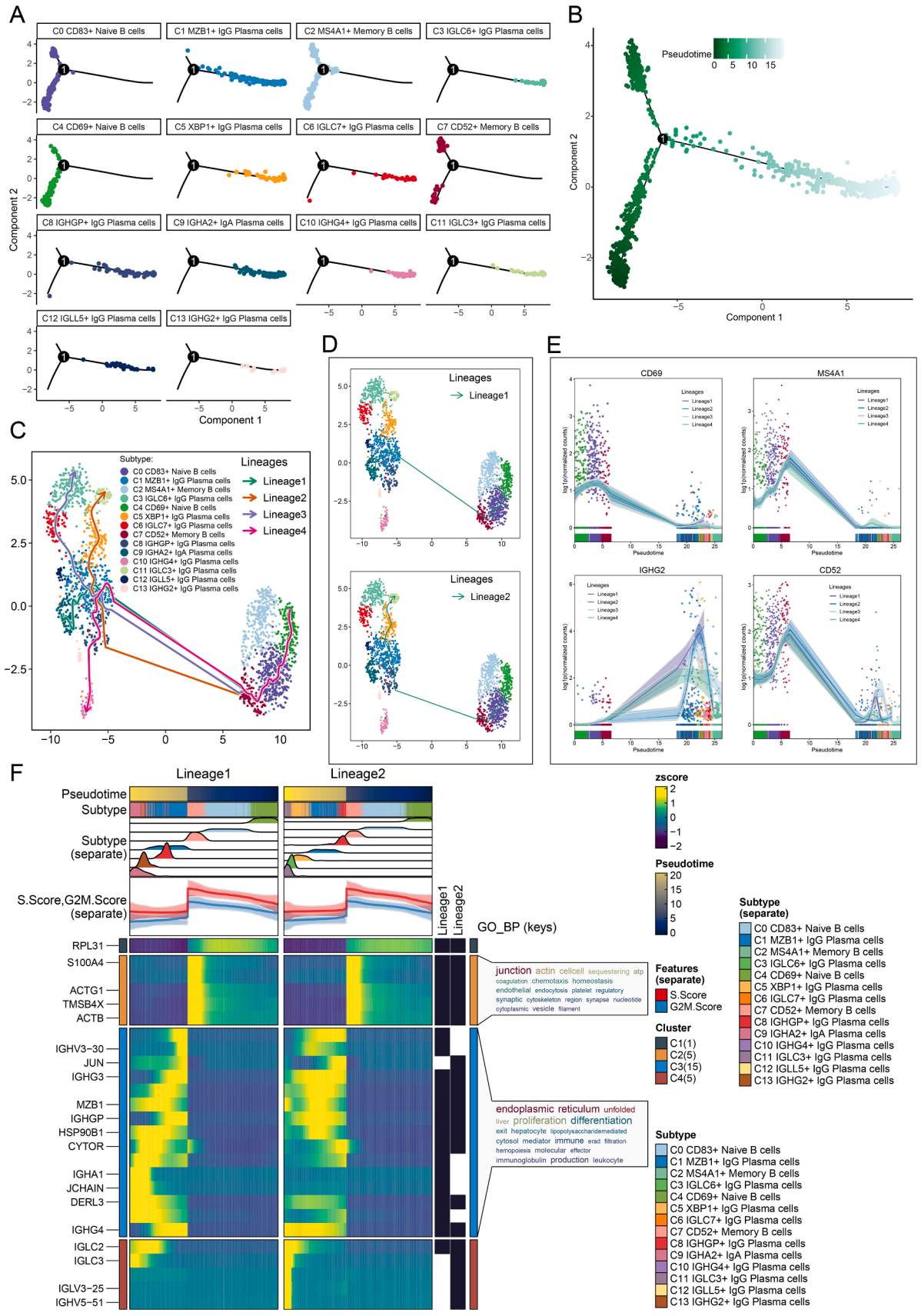

Figure 6. B and Plasma cell differentiation trajectories inferred by Monocle2 and Slingshot. (A) Pseudotime trajectory analysis of 14 B and Plasma cell subtypes based on Seurat clustering. (B) Monocle2 trajectory analysis based on Seurat clustering. (C) Distribution of differentiation trajectories of 14 B and Plasma cell subtypes. (D) Pseudotime trajectories of distinct differentiation lineages across 14 B and Plasma cell subtypes. (E) Dynamic expression of key genes (MS4A1, CD52, IGHG2, CD69). (F) Pseudotime multi-dimensional feature analysis of B and Plasma cell differentiation lineages (Lineage1, Lineage2).

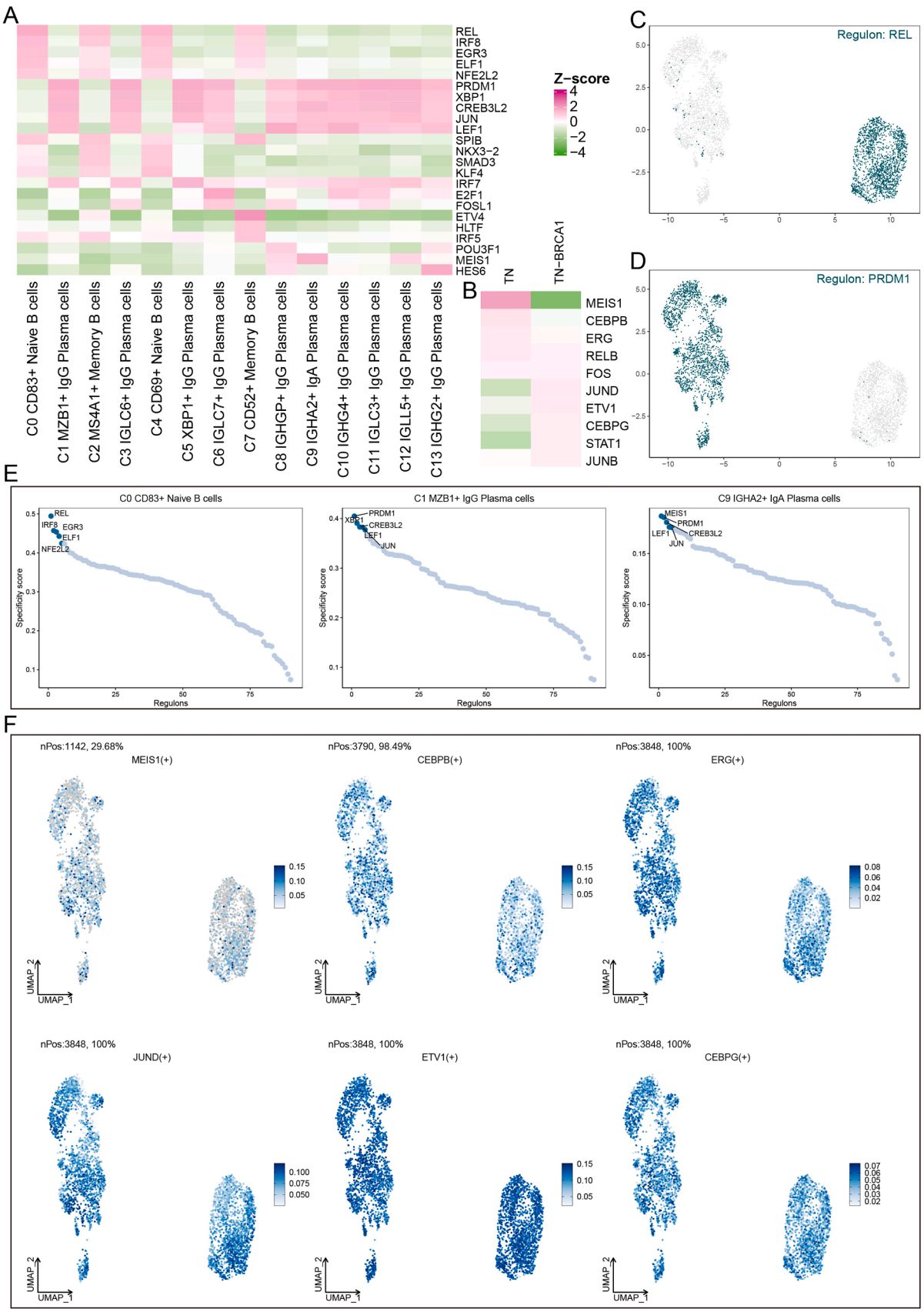

Figure 7. Transcription factor landscape of B and Plasma cell subtypes in TN and TN-BRCA1 tumors. (A) Heatmap showing transcription factor expression across 14 B and Plasma cell subtypes. (B) Heatmap showing transcription factor expression across the TN and TN-BRCA1 groups. (C-D) UMAP plot showing the distribution of transcriptional factors REL and PRDM1. (E) Transcriptional factors highly expressed in C0, C1 and C9 cell subtypes. (F) UMAP plot showing the distribution of transcription factors (MEIS1,CEBPB,ERG,JUND,ETV1 and CEBPG).

necessitates further validation. Furthermore, Figs. 7C-D depicted the expression distribution of certain transcription factors on the UMAP plot, indicating notable differential expression. TFs activity ranking revealed that the top three factors in C0 naïve B cells were *REL, IRF8*, and *EGR3*; in C1 IgG plasma cells, they were primarily *PRDM1, XBP1*, and *CREB3L2*; while in C9 IgA plasma cells, *MEIS1, PRDM1*, and *CREB3L2* dominated (Fig. 7E). These findings further validated the differentiation continuity and functional specificity of distinct B cell subtypes at the transcriptional regulatory level. Finally, Fig. 7F illustrated the expression distribution of TFs highly expressed in the TN group (*MEIS1, CEBPβ, ERG*) and those highly expressed in the TN-BRCA1 group (*JUND, ETV1, CEBPG*) on the UMAP plot.

Discussion

In this study, we constructed a breast cancer immune microenvironment atlas based on single-cell transcriptome technology, which has been proven to be a key method for resolving tumor immune heterogeneity [52–55]. We systematically compared the immune cell composition, functional status, and differentiation trajectory of common TNBC and BRCA1-mutated TNBC. We found that although the two belonged to TNBC at the receptor subtyping level, they showed significant differences in the immune ecological structure, especially in the composition and functional bias of the B cell lineage [33,56]. This discovery provided a new perspective for understanding the differences in immunotherapy responses among different TNBC subtypes.

Previous studies have generally believed that BRCA1-mutated TNBC was more sensitive to immunotherapy, mainly because the homologous recombination repair defect leaded to high mutation load, genomic instability and increased neoantigens [57,58]. In addition, BRCA1-mutated TNBC was often accompanied by higher levels of tumor-infiltrating lymphocytes, a feature that was closely related to the efficacy of ICIs [59,60]. Nevertheless, the mutation burden alone cannot entirely account for the variations in immunotherapy response; the cellular state and functional composition of the tumor immune microenvironment were also crucial factors.

In addition to the intrinsic genomic characteristics of tumors, the differentiation status and functional composition of immune cells, especially the state heterogeneity of B cells, may also be important factors in determining the efficacy of immunotherapy [61–63]. The current view was that B cells may play both pro-tumor and anti-tumor roles, depending on their phenotype, secreted antibodies, and surrounding TME [64,65]. These controversial results may be attributed to the heterogeneity of B cell subtypes and functions in different types of breast cancer. With the recent approval of immunotherapeutic agents as treatment options for patients with TNBC in early and metastatic stages, B cell populations or tertiary lymphoid structures (TLS) may become valuable biomarkers for immunotherapeutic responses in certain breast cancer subsets [66].

Our study found that naïve B cells and memory B cells were significantly enriched in BRCA1-mutated TNBC, while ordinary TNBC was dominated by terminally differentiated plasma cells. In recent years, a number of studies have shown that naïve and memory B cells were key components of TLS, and the formation of TLS is significantly associated with the efficacy of ICIs in a variety of solid tumors. In TNBC, the presence of TLS was considered an important biological marker for predicting immunotherapy response and long-term survival [67]. It was worth emphasizing that the difference in B cell status is often closely coupled with TLS. TLSs was considered tumor-localized "lymph node--like" structures that can promote antigen presentation, T cell initiation, and humoral immune maturation, and their presence usually indicates a more "mobilizable" immune microenvironment [68]. In TNBC, TLS has been shown to have prognostic value [69], and evidence is accumulating that TLS maturity or heterogeneity is associated with treatment response. Evidence from the broader field of cancer immunotherapy also supports the critical role of TLS and B cells in response to immune checkpoint blockade therapy, with Helmink et al. finding that TLS-related B cell features were significantly associated with response in a multi-cancer ICB cohort [70]. Therefore, BRCA1-mutated TNBCs showed a greater enrichment of naïve and memory B cells, suggesting that these tumors may provide a cellular context more conducive to TLS formation, thus making it easier to form an effective immune initiation and amplification circuit in ICB therapy. Therefore, the B cell state enriched in BRCA1-mutated TNBC may provide a more favorable immunological basis for immunotherapy.

In contrast, the dominance of plasma cells in common TNBC did not necessarily equate to "stronger anti-tumor". Plasma cells can exhibit a dual role in different tumors: in some cases, they indicate active humoral immunity and better prognosis, while in other cases, they may be coupled with immunosuppressive ecology. Classical mechanistic studies have shown that IgA+ plasma cells can inhibit CTL-mediated anti-tumor immunity by expressing PD-L1 and secreting IL-10, leading to treatment resistance [71,72]; in the context of chronic inflammation-related tumorigenesis, the accumulation of IgA+ cells can also weaken anti-tumor immune surveillance [73]. It was worth noting that this study observed an increase in the proportion of IgA plasma cells in ordinary TNBC, accompanied by a significant up-regulation of the transcription factor MEIS1. Therefore, if IgA plasma cells were enriched and terminally differentiated in common TNBC, it may mean that the immune response was more inclined to "regulatory or exhausted humoral immunity", thus limiting the reactivation effect of ICB on cytotoxic immunity. This feature may partially explain the poor response of ordinary TNBC to immunotherapy in clinical practice.

In addition to the differences in the composition of immune cells, this study further revealed the essential differences between the two types of TNBC from the perspective of cell differentiation plasticity. Previous studies have confirmed that the differentiation state and stemness characteristics of immune cells are of great significance in determining the persistence of immune response [74]. The naïve and memory B cells enriched in BRCA1-mutated TNBCs showed higher expression levels of pluripotency-related genes such as CD44, CTNNB1, and HIF1A, and had higher CytoTRACE scores, suggesting that they were in a lower differentiation and more plastic immune state, thereby playing a role in T cell activation. In contrast, plasma cells enriched in TNBC showed obvious terminal differentiation characteristics and lacked the potential for state transition. Previous studies have also shown that B cells in TNBC tend to differentiate into plasma cells, playing a role in humoral immunity [75]. Transcriptional regulation analysis further supported the above conclusion. The transcription factors JUND and ETV1, which are enriched in BRCA1-mutated TNBC, were associated with immune activation and cell state plasticity [76,77], while MEIS1 and CEBPB, which are highly expressed in common TNBC, were mainly concentrated in the IgA plasma cell subgroup, suggesting that there are different transcriptional regulatory networks in B cells in different TNBC subtypes. This regulatory difference may profoundly affect the overall functional state of the tumor immune microenvironment and ultimately determine the degree of response to immunotherapy.

Conclusion

In summary, this study systematically revealed the key differences between common TNBC and BRCA1-mutated TNBC at the level of the immune microenvironment from single-cell resolution. We proposed that BRCA1-mutated TNBC presented an immune ecosystem dominated by naïve and memory B cells with strong antigen presentation ability and state plasticity, which was more conducive to the efficacy of ICIs; while ordinary TNBC tended to form a humoral immune state dominated by plasma cells, terminally differentiated and limited in plasticity, which may limit the effect of immunotherapy. These findings have important clinical implications. In the future, immunotyping based on B cell differentiation status rather than simple immune cell abundance may be used to optimize patient screening strategies for TNBC immunotherapy.

Furthermore, therapies aimed at the B cell differentiation pathway, such as enhancing TLS formation or obstructing premature plasma cell terminal differentiation, may offer novel therapeutic strategies to augment the efficacy of immunotherapy for prevalent TNBC. Further studies were needed to combine spatial transcriptome, functional experiments and clinical immunotherapy cohorts to further verify and transform the above mechanisms.

Funding statement

This research was supported by the National Natural Science Foundation of China Key Program (82,430,123), the Shandong Provincial Taishan Scholars Distinguished Expert Program (tstp20221166), and the National Administration of Traditional Chinese Medicine High-Level Key Discipline Construction Project (ZYYZDXK-2023,125).

CRediT authorship contribution statement

Qi Sun: Visualization, Data curation, Conceptualization. **Yuting Zhong:** Writing – review & editing, Conceptualization. **Changgang Sun:** Supervision, Funding acquisition, Conceptualization.

Declaration of competing interest

The authors declare that they have no conflicts of interest.

Acknowledgments

The authors would like to acknowledge that no specific support was received for this study.

References

[1] C. Zhang, et al., POP1 Facilitates proliferation in triple-negative breast cancer via m6A-dependent degradation of CDKN1A mRNA, Research 7 (2024) 0472.
[2] Y. Tang, et al., Dissection of FOXO1-induced LYPLAL1-DT impeding triple-negative breast cancer progression via mediating hnRNPK/β-catenin complex, Research 6 (2023) 0289.
[3] Z. Guo, et al., Tumor microenvironment and immunotherapy for triple-negative breast cancer, Biomark. Res. 12 (2024) 166.
[4] Y. Yin, et al., Novel combination therapy for triple-negative breast cancer based on an intelligent hollow carbon sphere, Research 6 (0098) (2023).
[5] M.A. Harris, et al., Towards targeting the breast cancer immune microenvironment, Nat. Rev. Cancer 24 (2024) 554–577.
[6] Z. Zhao, et al., Ectopic expression of GDF15 in cancer-associated fibroblasts enhances melanoma immunosuppression via the GFRAL/RET cascade, J. ImmunOther Cancer 13 (2025) e011036.
[7] R. Xu, et al., Armored and cold tumors: a refractory subset of solid cancer, BIO Integr. 6 (2025) 1–6.
[8] Q. Cui, et al., DNA damage chemotherapeutic drugs suppress basal-like breast cancer growth by down-regulating the transcription of the FOXO1-KLF5 axis, Genes. Dis. 11 (2023) 91–94.
[9] M. Yang, et al., Tumor cell membrane-based vaccines: a potential boost for cancer immunotherapy, Exploration 4 (2024) 20230171.
[10] Q. Guo, et al., Antigen/adjuvant-free liposome induces adjuvant effects for enhancing cancer immunotherapy, Exploration 5 (2024) 20230115.
[11] S. Du, et al., Adoptive cell therapy for cancer treatment, Exploration 3 (2023) 20210058.
[12] L. Zhang, et al., Exploring cellular diversity in lung adenocarcinoma epithelium: advancing prognostic methods and immunotherapeutic strategies, Cell Proliferat. 57 (2024) e13703.
[13] G. Li, et al., Breaking boundaries: chronic diseases and the frontiers of immune microenvironments, Med. Res. 1 (2025) 62–102.
[14] Y. Abdou, et al., Immunotherapy in triple negative breast cancer: beyond checkpoint inhibitors, NPJ. Breast. Cancer 8 (2022) 121.
[15] Z. Zhou, Q. Zhou, Immunotherapy resistance in triple-negative breast cancer: molecular mechanisms, tumor microenvironment, and therapeutic implications, Front. Oncol. 15 (2025) 1630464.
[16] R. Feng, A. Gu, G. Zengin, M. Du, Low-intensity pulsed ultrasound enhances NK cell adoptive therapy by modulating the wnt/β-catenin signaling pathway, BIO Integr. 6 (2025) 1–8.
[17] J. Niu, et al., Novel CAR-T cells specifically targeting Nectin4 exhibit effective anti-tumor efficacy in bladder cancer cell lines, BIO Integr. 6 (2025) 1–11.
[18] G. Lai, et al., The characteristics of tumor microenvironment predict survival and response to immunotherapy in adrenocortical carcinomas, Cells 12 (2023) 755.
[19] G. Lai, et al., Identification and validation of a gene signature for lower-grade gliomas based on pyroptosis-related genes to predict survival and response to Immune checkpoint inhibitors, J. Heal. Eng. 2022 (2022) 8704127.
[20] E.P. Winer, et al., Pembrolizumab versus investigator-choice chemotherapy for metastatic triple-negative breast cancer (KEYNOTE-119): a randomised, open-label, phase 3 trial, Lancet Oncol. 22 (2021) 499–511.
[21] Y. Zhou, et al., Erratum to "tumor microenvironment-specific chemical internalization for enhanced gene therapy of metastatic breast cancer", Research 6 (2023) 0076.
[22] J. Xie, et al., Single-cell RNA sequencing elucidated the landscape of breast cancer brain metastases and identified ILF2 as a potential therapeutic target, Cell Proliferat. 57 (2024) e13697.
[23] H. Zhao, et al., Integrated analysis of single-cell and bulk RNA sequencing data reveals immune-related lncRNA-mRNA prognostic signature in triple-negative breast cancer, Genes. Dis. 11 (2023) 571–574.
[24] M. Zhang, et al., Engineering a pH-responsive polymeric micelle co-loaded with paclitaxel and triptolide for breast cancer therapy, Cell Proliferat. 57 (2024) e13603.
[25] S. Vinayak, et al., Open-label clinical trial of Niraparib combined with Pembrolizumab for treatment of advanced or metastatic triple-negative breast cancer, JAMA Oncol. 5 (2019) 1132–1140.
[26] W. Nie, et al., Single-cell RNA sequencing reveals the potential role of Postn(+) fibroblasts in promoting the progression of myocardial fibrosis after myocardial infarction, Sci. Rep.-UK 15 (2025) 22390.
[27] W. Ge, et al., Single-cell transcriptomics identifies FOSL1-regulated IGFBP3+ melanoma subtype as a neuro-immunoregulatory signaling hub facilitating tumor progression, Front. Immunol. 16 (2025) 1662869.
[28] W. Nie, J. Yan, Z. Xie, Y. Liu, J. Zhang, W. Yong, et al., Single-cell omics analysis reveals critical cell subtypes and their functional attributes in myocardial ischemia-reperfusion injury, Bio. Integr. (2026) 7, https://doi.org/10.15212/bioi-2025-015935.
[29] W. Tang, et al., Single-cell RNA-sequencing atlas reveals an FABP1-dependent immunosuppressive environment in hepatocellular carcinoma, J. ImmunOther Cancer 11 (2023) e007030.
[30] H. Du, et al., Single-cell RNA-seq and bulk-seq identify RAB17 as a potential regulator of angiogenesis by human dermal microvascular endothelial cells in diabetic foot ulcers, Burns. Trauma 11 (2023) tkad020.
[31] Y. Fang, et al., Systematic investigation of tumor microenvironment and antitumor immunity with IOBR, Med. Res. 1 (2025) 136–140.
[32] L. Xu, et al., A comprehensive single-cell breast tumor atlas defines epithelial and immune heterogeneity and interactions predicting anti-PD-1 therapy response, Cell Rep. Med. 5 (2024) 101511.
[33] Y. Xin, et al., Analysis of single-cell and spatial transcriptomics in TNBC cell-cell interactions, Front. Immunol. 16 (2025) 1521388.
[34] D. Wu, et al., Single-cell analyses revealed key tumor-infiltrating myeloid cell subsets associated with clinical outcomes in different subtypes of breast cancer, Genes. Dis. 11 (2023) 101185.
[35] B. Pal, Y. Chen, F.O. Vaillant, B.D. Capaldo, R. Joyce, X. Song, et al., A single-cell RNA expression atlas of normal, preneoplastic and tumorigenic states in the human breast, EMBO J. (2021) 40, https://doi.org/10.15252/embj.2020107333.
[36] Z. Zhao, et al., Cancer-associated fibroblast-derived GDF15 induces oxidative stress and neutrophil infiltration in head and neck squamous cell carcinoma through the PI3K/AKT/STAT3 axis cascade, Research 8 (2025) 0901.
[37] Q. Liu, et al., Cold-induced reprogramming of subcutaneous white adipose tissue assessed by single-cell and single-nucleus RNA sequencing, Research 6 (2023) 0182.
[38] X.C. Cheng, et al., Single-cell sequencing technology in skin wound healing, Burns. Trauma 12 (2024) tkae043.
[39] Y. Liu, M. Chen, L. Zhang, T. Lyu, Y. Geng, W. Li, et al., Comparisons in microglial responses to ischemic–hypoxic brain injury in neonatal and adult mice analyzed by transcriptome integration and deconvolution technologies, Adv. Technol. Neurosci. 2 (2025) 161–172, https://doi.org/10.4103/ATN.ATN-d-25-00004.
[40] Z. Xi, et al., Investigation of the effects of Si-A/PUE@HA hydrogels on the osteochondral defect microenvironment based on single-cell RNA sequencing, J. Nanobiotechnol. 23 (2025) 680.
[41] R. Hong, et al., eMCI: an explainable multimodal correlation integration model for unveiling spatial transcriptomics and intercellular signaling, Research 7 (2024) 0522.
[42] Y. He, et al., SHED-derived exosome-mimetics promotes rotator cuff tendon-bone healing via macrophage immunomodulation through NF-κb suppression and autophagy activation, Mater. Today Bio. 34 (2025) 102146.
[43] Y. Xia, et al., Decoding the molecular landscape of keloids: new insights from single-cell transcriptomics, Burns. Trauma 11 (2023) tkad017.
[44] A. Franken, et al., Single-cell transcriptomics identifies pathogenic T-helper 17.1 cells and pro-inflammatory monocytes in immune checkpoint inhibitor-related pneumonitis, J. ImmunOther Cancer 10 (2022) e005323.
[45] Y. He, et al., An injectable multi-functional composite bioactive hydrogel for bone regeneration via immunoregulatory and osteogenesis effects, Adv. Compos. Hybrid. Mater. 8 (2025) 128.
[46] P. Blanc, et al., Mature IgM-expressing plasma cells sense antigen and develop competence for cytokine production upon antigenic challenge, Nat. Commun. 7 (2016) 13600.
[47] B. Schröder, The multifaceted roles of the invariant chain CD74–more than just a chaperone, Biochim. Biophys. Acta 1863 (2016) 1269–1281.
[48] S. Liu, et al., Metabolic reprogramming and therapeutic resistance in primary and metastatic breast cancer, Mol. Cancer 23 (2024) 261.

[49] L. Versteeg, et al., Immunopeptidomic MHC-I profiling and immunogenicity testing identifies Tcj2 as a new Chagas disease mRNA vaccine candidate, PLoS. Pathog. 20 (2024) e1012764.
[50] C.M. Laumont, B.H. Nelson, IgA transcytosis: a new weapon in the immune response to cancer? Cancer Cell 39 (2021) 607–609.
[51] L. Miao, et al., Unraveling the dual roles of tumor-infiltrating antibodies in solid tumors: friend or foe in the tumor microenvironment? Front. Immunol. 16 (2025) 1671839.
[52] S. Olbrecht, et al., High-grade serous tubo-ovarian cancer refined with single-cell RNA sequencing: specific cell subtypes influence survival and determine molecular subtype classification, Genome Med. 13 (2021) 111.
[53] G. Gao, et al., Integration of bulk RNA sequencing and single-cell RNA sequencing to reveal uveal melanoma tumor heterogeneity and cells related to survival, Front. Immunol. 13 (2022) 898925.
[54] C. Chen, et al., LNMAT1 promotes lymphatic metastasis of bladder cancer via CCL2 dependent macrophage recruitment, Nat. Commun. 9 (2018) 3826.
[55] G. Lai, et al., A novel m7G-related genes-based signature with prognostic value and predictive ability to select patients responsive to personalized treatment strategies in bladder cancer, Cancers 14 (2022) 5346.
[56] S. Singh, et al., Chemotherapy coupled to macrophage inhibition induces T-cell and B-cell infiltration and durable regression in triple-negative breast cancer, Cancer Res. 82 (2022) 2281–2297.
[57] A. Tutt, et al., Carboplatin in BRCA1/2-mutated and triple-negative breast cancer BRCAness subgroups: the TNT Trial, Nat. Med. 24 (2018) 628–637.
[58] M.L. Telli, et al., Homologous recombination deficiency (HRD) score predicts response to platinum-containing neoadjuvant chemotherapy in patients with triple-negative breast cancer, Clin. Cancer Res.: Off. J. Am. Assoc. Cancer Res. 22 (2016) 3764–3773.
[59] K. Kang, et al., Homologous recombination deficiency in triple-negative breast cancer: multi-scale transcriptomics reveals distinct tumor microenvironments and limitations in predicting immunotherapy response, Comput. Biol. Med. 158 (2023) 106836.
[60] S. Sun, et al., Resolving tumor microenvironment heterogeneity to forecast immunotherapy response in triple-negative breast cancer through multi-scale analysis, Front. Oncol. 15 (2025) 1538574.
[61] L. Lin, et al., Germinal center B-cell subgroups in the tumor microenvironment cannot be overlooked: their involvement in prognosis, immunotherapy response, and treatment resistance in head and neck squamous carcinoma, Heliyon 10 (2024).
[62] H. Li, et al., The cellular signaling crosstalk between memory B cells and tumor cells in nasopharyngeal carcinoma cannot be overlooked: their involvement in tumor progression and treatment strategy is significant, J. Cancer 16 (2025) 288–314.
[63] B. Pellegrino, et al., CD74 promotes the formation of an immunosuppressive tumor microenvironment in triple-negative breast cancer in mice by inducing the expansion of tolerogenic dendritic cells and regulatory B cells, PLoS. Biol. 22 (2024) e3002905.
[64] G.V. Sharonov, et al., B cells, plasma cells and antibody repertoires in the tumour microenvironment, Nat. Rev. Immunol. 20 (2020) 294–307.
[65] Z. Gao, et al., Heterogeneity of intratumoral microbiota within the tumor microenvironment and relationship to tumor development, Med. Res. 1 (2025) 32–61.
[66] M. Li, et al., B cells in breast cancer pathology, Cancers 15 (2023) 1517.
[67] Q. Wang, et al., Heterogeneity of tertiary lymphoid structures predicts the response to neoadjuvant therapy and immune microenvironment characteristics in triple-negative breast cancer, Brit. J. Cancer 132 (2025) 295–310.
[68] S. Jiao, et al., Intratumor expanded T cell clones can be non-sentinel lymph node derived in breast cancer revealed by single-cell immune profiling, J. ImmunOther Cancer 10 (2022) e003325.
[69] F. Boissière-Michot, et al., Prognostic value of tertiary lymphoid structures in triple-negative breast cancer: integrated analysis with the tumor microenvironment and clinicopathological features, Front. Immunol. 15 (2024) 1507371.
[70] B.A. Helmink, et al., B cells and tertiary lymphoid structures promote immunotherapy response, Nature 577 (2020) 549–555.
[71] S. Shalapour, et al., Immunosuppressive plasma cells impede T-cell-dependent immunogenic chemotherapy, Nature 521 (2015) 94–98.
[72] G. Lai, et al., Comprehensive analysis of immune subtype characterization on identification of potential cells and drugs to predict response to immune checkpoint inhibitors for hepatocellular carcinoma, Genes. Dis. 12 (2024) 101471.
[73] S. Shalapour, et al., Inflammation-induced IgA+ cells dismantle anti-liver cancer immunity, Nature 551 (2017) 340–345.
[74] I. Siddiqui, et al., Intratumoral Tcf1(+)PD-1(+)CD8(+) T cells with stem-like properties promote tumor control in response to vaccination and checkpoint blockade immunotherapy, Immunity 50 (2019) 195–211, e10.
[75] S. Ding, et al., Single-cell atlas reveals a distinct immune profile fostered by T?Cell-B?Cell crosstalk in triple negative breast cancer, Cancer Commun. Lond. Engl. 43 (2023) 661–684.
[76] M. Yan, et al., Dynamic regulatory networks of T cell trajectory dissect transcriptional control of T cell state transition, Mol. Ther. Nucleic. Acids. 26 (2021) 1115–1129.
[77] J. Behmoaras, et al., Jund is a determinant of macrophage activation and is associated with glomerulonephritis susceptibility, Nat. Genet. 40 (2008) 553–559.